



Heriot-Watt University  
Research Gateway

## Unmodified multi-wall carbon nanotubes in polylactic acid for electrically conductive injection-moulded composites

### Citation for published version:

Rivière, P, Nypelö, TE, Obersriebnig, M, Bock, H, Müller, M, Mundigler, N & Wimmer, R 2016, 'Unmodified multi-wall carbon nanotubes in polylactic acid for electrically conductive injection-moulded composites', *Journal of Thermoplastic Composite Materials*. <https://doi.org/10.1177/0892705716649651>

### Digital Object Identifier (DOI):

[10.1177/0892705716649651](https://doi.org/10.1177/0892705716649651)

### Link:

[Link to publication record in Heriot-Watt Research Portal](#)

### Document Version:

Peer reviewed version

### Published In:

Journal of Thermoplastic Composite Materials

### General rights

Copyright for the publications made accessible via Heriot-Watt Research Portal is retained by the author(s) and / or other copyright owners and it is a condition of accessing these publications that users recognise and abide by the legal requirements associated with these rights.

### Take down policy

Heriot-Watt University has made every reasonable effort to ensure that the content in Heriot-Watt Research Portal complies with UK legislation. If you believe that the public display of this file breaches copyright please contact [open.access@hw.ac.uk](mailto:open.access@hw.ac.uk) providing details, and we will remove access to the work immediately and investigate your claim.

**Unmodified multi-wall carbon nanotubes in polylactic acid  
for electrically-conductive injection moulded composites**

Journal:	<i>Journal of Thermoplastic Composite Materials</i>
Manuscript ID:	JTCM-15-0172.R1
Manuscript Type:	Original Manuscript
Date Submitted by the Author:	15-Mar-2016
Complete List of Authors:	Rivière, Pauline; Institute of Natural Materials Technology, Department of Agrobiotechnology, IFA-Tulln Nypelö, Tiina; Division of Chemistry of Renewable Resources, Department of Chemistry Bock, Henry; Institute of Chemical Sciences, Department of Engineering & Physical Sciences Müller, Marcus; University of Applied Forest Sciences Obersriebnig, Michael; Institute of Wood Technology and Renewable Materials, Department of Material Sciences and Process Engineering Mundigler, Norbert; Institute of Natural Materials Technology, Department of Agrobiotechnology, IFA-Tulln Wimmer, Rupert; Institute of Natural Materials Technology, Department of Agrobiotechnology, IFA-Tulln
Keywords:	Carbon nanotubes, thermoplastics, PLA, MWCNT, injection moulding, electrical conductivity, AFM, crystallization, melt mixing
Abstract:	Tailoring the properties of natural polymers such as electrical conductivity is vital to widen the range of future applications. In this paper the potential of electrically conducting multi-wall carbon nanotube/polylactic acid composites produced by industrially viable melt mixing is assessed simultaneously to MWCNT influence on the composite's mechanical strength and polymer crystallinity. Atomic force microscopy observations showed that melt mixing achieved an effective distribution and individualisation of unmodified nanotubes within the polymer matrix. However, as a trade-off of the poor tube/matrix adhesion the tensile strength was lowered. With 10 wt% MWCNT loading the tensile strength was 26% lower than for neat PLA. Differential scanning calorimetric measurements indicated that polymer crystallization after injection moulding was nearly unaffected by the presence of nanotubes, and remained at 15%. The resulting composites became conductive below 5 wt% loading and reached conductivities of 51 S/m at 10 wt%, which is comparable with conductivities reported for similar nanocomposites obtained at lab-scale.

SCHOLARONE™  
Manuscripts

For Peer Review

1  
2  
3  
4  
5  
6  
7  
8  
9  
10  
11  
12  
13  
14  
15  
16  
17  
18  
19  
20  
21  
22  
23  
24  
25  
26  
27  
28  
29  
30  
31  
32  
33  
34  
35  
36  
37  
38  
39  
40  
41  
42  
43  
44  
45  
46  
47  
48  
49  
50  
51  
52  
53  
54  
55  
56  
57  
58  
59  
60

*Original Article***Unmodified multi-wall carbon nanotubes in polylactic acid for electrically-conductive injection moulded composites**

**Pauline Rivière<sup>1</sup>, Tiina E Nypelö<sup>2</sup>, Michael Obersriebnig<sup>3</sup>, Henry Bock<sup>4</sup>, Marcus Müller<sup>5</sup>, Norbert Mundigler<sup>1</sup> and Rupert Wimmer<sup>1,3</sup>**

<sup>1</sup>Department of Agrobiotechnology, Institute of Natural Materials Technology, IFA-Tulln, University of Natural Resources and Life Sciences, Tulln A-3430, Austria

<sup>2</sup>Department of Chemistry, University of Natural Resources and Life Sciences, Vienna A-1190, Austria

<sup>3</sup>Department of Material Sciences and Process Engineering, Institute of Wood Science and Technology, University of Natural Resources and Life Sciences, Vienna A-1190, Austria

<sup>4</sup>Institute of Chemical Sciences, Heriot Watt University, Edinburgh, United Kingdom

<sup>5</sup>University of Applied Forest Sciences Rottenburg, Schadenweilerhof, 72108 Rottenburg am Neckar, Germany

Corresponding author:

Rupert Wimmer, Department of Agrobiotechnology, Institute for Natural Materials Technology, IFA-Tulln, University of Natural Resources and Life Sciences, Tulln A-3430, Austria.

Email: rupert.wimmer@boku.ac.at

1  
2  
3  
4  
5  
6  
7  
8  
9  
10  
11  
12  
13  
14  
15  
16  
17  
18  
19  
20  
21  
22  
23  
24  
25  
26  
27  
28  
29  
30  
31  
32  
33  
34  
35  
36  
37  
38  
39  
40  
41  
42  
43  
44  
45  
46  
47  
48  
49  
50  
51  
52  
53  
54  
55  
56  
57  
58  
59  
60

*Original Article*

**Unmodified multi-wall carbon nanotubes in polylactic acid for electrically-conductive injection moulded composites**

**INTRODUCTION**

Polylactid acid (PLA) is a promising bio-based and biodegradable thermoplastic, envisioned to increasingly replace oil-based plastics. It has already been successfully established for applications ranging from textiles, medical appliances to food packaging.<sup>1,2</sup> The demand for bio-based polymers is expected to grow significantly during the next few years. Based on 2012 capacities, the bioplastic production in Europe has been forecasted to increase 400 % by 2017.<sup>3</sup> Plastics are generally electrically insulating materials (specific volume conductivity  $\sigma < 10^{-9}$  S/m), due to the very low conductivity of their polymer matrices.<sup>4</sup> As a consequence, electrical charges may accumulate at plastic product surfaces resulting in detrimental effects that range from the electrostatic attraction of dust to the induction of electrical shocks to handlers and electronic systems. To prevent the accumulation of surface charges, the conductivity of the material must be larger than  $10^{-9}$  S/m, which classifies them as electrostatic dissipative materials.<sup>1</sup> Various additives and treatments have been developed to increase the conductivity of oil-based polymers above this limit.<sup>4</sup> Achieving the same for biopolymers, i.e. controlling the electrical conductivity of biopolymers, is essential to enable a much broader range of applications spanning from packaging of electronic items and dangerous goods containers, to automotive components.<sup>1,4-8</sup>

Conducting fillers such as carbon fibres (CF), carbon black (CB), metallic fibres and powders, as well as powders of layered minerals, are commonly used to enhance the permanent conductivity of composites.<sup>4</sup> Depending on filler type and loading, the

composites can reach conductivities above  $10^{-3}$  S/m and thereby enter the group of electrically conductive materials.<sup>4</sup> Recent research on conductive composites has been focused on the utilization of carbon-based nanofillers, especially on carbon nanotubes (CNTs).<sup>9-11</sup> Carbon nanotubes are particularly attractive as they combine many outstanding properties including mechanical strength and stiffness as well as thermal and electrical conductivities that are superior to most other fillers.<sup>12-14</sup> Additionally, their high aspect ratio (length/diameter, typically up to 10 000) leads to particularly low electrical percolation thresholds, offering [also](#) a large surface area to interact with the matrix.<sup>13-14</sup>

The preparation of electrically conducting materials based on CNTs has been described.<sup>4,15</sup> It was found that to achieve the desired high conductivities a good dispersion of the carbon nanotubes in the polymer matrix is critical. Poor dispersion resulting from bundling and entanglement of the CNTs leads to unnecessarily high percolation thresholds, leading to CNT wastage and poor composite homogeneity.<sup>16</sup> For optimal CNT dispersion various preparation methods have been tested among which melt processing is the most suitable for industry.<sup>15,17</sup> During melt processing high shear forces are applied to the material by a co-rotating twin-extruder.<sup>15</sup> Shear forces can be increased by using high rotation speeds and highly viscous mixtures.<sup>15</sup> The latter is exploited by loading the polymer with higher concentrations of CNTs to produce masterbatches, followed by diluting them with pure polymer to the desired concentration.<sup>15,17</sup>

Whilst the degree of dispersion of the filler is mostly determined by the processing of the melt, subsequent shaping processes may also have an effect on the properties of the resulting composite.<sup>16,17</sup> Different shaping processes such as injection moulding, compression moulding, extrusion and film blowing can be employed depending on the object to be produced. Injection moulding is known as one of the most common procedures

1  
2  
3  
4  
5  
6  
7  
8  
9  
10  
11  
12  
13  
14  
15  
16  
17  
18  
19  
20  
21  
22  
23  
24  
25  
26  
27  
28  
29  
30  
31  
32  
33  
34  
35  
36  
37  
38  
39  
40  
41  
42  
43  
44  
45  
46  
47  
48  
49  
50  
51  
52  
53  
54  
55  
56  
57  
58  
59  
60

in industry.<sup>18</sup> An interesting example is mentioned by Pegel et al.<sup>16</sup> where injection moulding with CNT at low pressing speed and high temperatures was performed. They observed secondary CNT agglomeration during pressing, which also induced an increase in electrical conductivity of the composites due to improved contacts between the CNTs.<sup>16,19</sup>

Another critical issue for CNT-composite manufacturing is the interaction between the filler and the polymer.<sup>20-23</sup> Filler-polymer adhesion can be improved by using polymers with higher affinity to the filler or by CNT surface modifications such as grafting and oxidation.<sup>2,17,22-23</sup> In general, improved filler-matrix adhesion leads to improved CNT dispersion and enhanced mechanical properties.<sup>2,17</sup> However, aggressive surface treatment such as oxidation degrades the CNTs and therefore compromises their properties. Thus, on one hand, chemical modification of the CNT surfaces enables good dispersion of the tubes in the polymer matrix, which shifts the practical electrical percolation threshold towards a lower loading. On the other hand, chemical modification requires an additional and complex processing step, and may decrease the aspect ratio of the MWCNT and hinder the -direct leading to fewer contacts between the nanotubes. As a consequence, percolation threshold may increase, which degrades electrical conductivity of the composite.<sup>17,24</sup>

Most of the prevalent literature on carbon nanotube-PLA thermoplastic composites is concerned with the effects of surface modification of multi-wall carbon nanotubes (MWCNTs) on material properties and the development of mixing processes.<sup>19,25-26</sup> MWCNTs are attractive as they are the cheapest type of CNT to produce, and they offer the opportunity of surface modification without detrimental effects on the inner layers.<sup>10,11,13</sup> However, surface modification may not be necessary to sufficiently disperse the tubes in the polymer matrix as shown in the studies by Mack et al.<sup>22</sup>, Villmow et al.<sup>15</sup> and Novais et al.<sup>27</sup>. These authors used unmodified MWCNTs in polycarbonate and PLA to produce composites

by melt mixing followed by compression moulding or injection moulding, obtaining reasonable dispersion and electrical conductivities. Novais et al.<sup>27</sup> even obtained higher conductivities on compressed plates when adding unmodified MWCNTs to PLA instead of PLA-grafted MWCNTs. This is consistent with the hypothesis that grafting hinders electrical tube/tube contacts.

MWCNT have also been demonstrated to influence the crystallization of semi-crystalline thermoplastics. The relatively low crystallization rate make the PLA more elastic, which is of interest for blow-forming and film production processes.<sup>28-29</sup> However, for the production of technical plastics, crystallinity closer to the maximal crystallinity of PLA is preferred, as it is associated with a higher glass transition temperature, improved thermal resistance, enhanced barrier properties, and higher mechanical strength.<sup>28-29</sup> Of particular interest is to maximize the crystallinity of plastic materials during high productivity production processes, for which the cooling time is minimized.<sup>28</sup> Therefore, the ability of different nanofillers, including multi-walled carbon nanotubes (MWCNT), to nucleate PLA crystallization has been studied.<sup>11,17,21,28-32</sup> Through nucleation the formation of numerous and more homogenous repartitions of spherulites are induced throughout the composite.<sup>29</sup> Zhang et al.<sup>33</sup> could demonstrate the nucleation effect of MWCNTs but also reported that crystallization would affect the MWCNT environment in various ways. On the one hand, some studies explained that when MWCNTs act as a nucleating agent, their surface will be covered by a crystalline polymer layer.<sup>17,15,25,34-35</sup> This is of importance when using MWCNT to build a conductive network in a semi-crystalline polymer as it could prevent direct contact between the MWCNTs and thereby hinder the transfer of electrons through the composite.<sup>17,35,18</sup> On the other hand, other studies described that the MWCNTs were more present in amorphous regions after crystallisation.<sup>1,25</sup> Leute<sup>4</sup> explains that in semi-crystalline polymers, nanosized



1  
2  
3  
4  
5  
6  
7  
8  
9  
10  
11  
12  
13  
14  
15  
16  
17  
18  
19  
20  
21  
22  
23  
24  
25  
26  
27  
28  
29  
30  
31  
32  
33  
34  
35  
36  
37  
38  
39  
40  
41  
42  
43  
44  
45  
46  
47  
48  
49  
50  
51  
52  
53  
54  
55  
56  
57  
58  
59  
60

fillers such as carbon black are excluded from the crystalline regions during crystallization and remain in amorphous regions.

Only few researchers related the electrical conductivity of nanocomposites to its crystallinity.<sup>31,35</sup> Among them, Alig et al.<sup>35</sup> found that through annealing (between 210 and 220°C for less than 15min) MWCNT-polypropylene composites, increased conductivity of the composites could be reached. To our knowledge, the present study is the first one characterizing the effect of unmodified MWCNT on electrical conductivity, with simultaneous measurements of the polymer crystallinity and the mechanical properties of injection moulded PLA-based composites. As no modification of the MWCNT surface was performed, the interaction between MWCNT and the polymer matrix is supposed to be weak.<sup>30,32</sup> Therefore we expect a decrease in tensile strength as the content of MWCNT is increasing, as observed before by e.g. Yoon et al.<sup>32</sup>. We suggest that the MWCNT are having a nucleation effect on the PLA crystallization after injection moulding, which affects MWCNT distribution and thereby the electrical conductivity of the composite. Through our research we are suggesting an industrially viable way of processing electrically conductive and injection moulded nanocomposites.

**EXPERIMENTAL**

NatureWorks® Ingeo™ 3251D Injection grade PLA was used. This PLA type has a melt flow index (MFI) of 70-85 g/10min (at 210 °C/2.16kg; ASTM D1238) and a density of 1.24 g/cm<sup>3</sup> (ASTM D792). With the low D –isomer content of 1.40 ±0.20 % higher crystallinity levels are anticipated.

-Multi-wall carbon nanotubes (MWCNTs) were provided by a local supplier as a powder. The MWCNTs were produced through catalytic chemical vapour deposition process followed by

separation of the CNTs from the catalyst by rinsing with citric acid and subsequent drying between 600 and 1000 °C. The amount of the metal catalyst remaining after purification was monitored by thermogravimetric analysis under air. A mean residual mass of 3 wt %  $\pm$  1.2 at 700 °C was determined from five MWCNT samples. According to the supplier the tubes had a diameter of less than 50 nm and their average length varied between 1-20  $\mu$ m. This was further confirmed by scanning electron microscopy (SEM) using the FEI Inspect S50 environmental SEM with a Tungsten gun. The dimensions were determined using ImageJ64 software and an average diameter of 38 nm  $\pm$  10 nm was found for 45 randomly selected MWCNTs. It was difficult to assess the length of the nanotubes as they were entangled but the observable length was found to be higher than 1  $\mu$ m for all tubes. MWCNTs had a density between 1.6 and 1.8 g/cm<sup>3</sup>. The specific electrical conductivity of the individual MWCNTs as given by the producer was 10<sup>5</sup> to 10<sup>6</sup> S/m with a maximum electric current density of up to 10<sup>13</sup> A/cm<sup>2</sup>.

A 10 kg masterbatch of 15 wt% MWCNT in PLA was produced by mixing dry MWCNTs with melted PLA in a ZSE 27MAXX extruder (Leistritz) equipped with co-rotating screws (MAXX 40 D) suitable for nanomaterials compounding. The used rotation speed was 450 rpm, and the temperature profiles were set between 200 and 230 °C. The masterbatch was diluted with neat PLA to a MWCNT content of 0, 0.5, 1, 2.5, 5, 7.5 and 10 wt% through melt mixing using a miniature Collin® ZK25 counter-rotating twin screw extruder. During the second extrusion step the melt temperature was kept constant at 175 °C and the pressure measured at the output varied between 24 and 42 bar. The extruded strands were cut into granules (length 4 $\pm$ 2 mm) for further processing. To limit sticking of the granules in the injection moulding feeding zone, the PLA crystallinity was increased by thermal annealing for 4 hours at 120 °C and subsequent storage at 80 °C to avoid water uptake. Bars were injected following the

1  
2  
3  
4  
5  
6  
7 standard ISO 179/1eU specifications on a Battenfeld™ HM 60/210 with the barrel  
8  
9 temperature set to 180 °C. Injection pressure varied between 631 and 996 bar and injection  
10  
11 145 temperature was kept constant at 175 °C. Prior to testing, tests bars were stored in a climate  
12  
13 room at 23 °C and 50 % relative humidity for 2 weeks.

14  
15 **Scanning electron microscopy (SEM)**

16  
17 The pure nanotubes were observed with a scanning electron microscope FEI Inspect S50®  
18  
19 under high vacuum mode, using 15 kV acceleration voltage and a medium spot size of 3 mm.  
20  
21 This SEM and a Quanta™ 250 FEG SEM were used to observe fractured surfaces of the  
22 150  
23 composites after tensile tests.

24  
25 **Atomic Force Microscopy (AFM)**

26  
27 AFM images of sample cross-sections of the injection moulded composites were acquired to  
28  
29 investigate dispersion and distribution of the MWCNTs in the matrix. Cross-section surfaces  
30  
31 for AFM imaging were prepared with a diamond knife mounted in an ultramicrotome. AFM  
32 155  
33 measurements were performed using a Veeco® Dimension Icon scanning probe microscope  
34  
35 with ScanAsyst™ in tapping mode. Soft tapping mode Al coated probes with a force constant  
36  
37 of 5 N/m and tip radius of <10 nm were used. Images on minimum 5 different locations were  
38  
39 recorded on each sample. Topography images were complemented by phase images to  
40  
41 visualize surface stiffness. Stiffer regions show a more positive phase shift and therefore  
42 160  
43 appear lighter in the phase images.<sup>36</sup>

44  
45 **Mechanical properties**

46  
47 Tensile tests were carried out on a Zwick-Roell ZmartPro, following ISO 527. Charpy  
48  
49 unnotched impact tests were conducted following ISO 179/1eU. Each test was repeated ten  
50  
51 times. Mean values are plotted with the corresponding standard deviation.  
52  
53 165

### Polymer crystallinity

The effect of MWCNT on polymer crystallization was assessed by a [differential scanning calorimetry \(DSC\)](#) 200 F3 Maia® (Netzsch). Measurements were done on three samples for each compound containing 0, 1, 2.5, 5 and 10 wt% MWCNT. The samples for crystallinity determination were cut from the tensile test bars, with masses between 5 mg and 15 mg, and were then placed into the aluminium DSC pans. Samples were heated and cooled twice under N<sub>2</sub> atmosphere, between 25°C and 200°C, at a heating rate of 10°C/min. Crystallinities were calculated following [Equation \(1\)](#) and indicated by Xc1 and Xc2 for the first and second heating step, respectively.

$$X_c(\%) = \frac{\Delta H_m - \Delta H_c}{\Delta H_m^0 \times \omega} \quad (1)$$

In [Equation \(1\)](#)  $\Delta H_m^0$  is the melting enthalpy of 100% crystalline PLA, for which a value of 93.7 J/g was used<sup>28,37,38</sup>,  $\Delta H_m$  represents the measured melting enthalpy of the sample<sup>37</sup>,  $\omega$  is the PLA mass fraction and  $\Delta H_c$  the post crystallization enthalpy.

### Polarized light microscopy

Polarized light microscopy was used to determine the position and amount of crystalline regions in the composites depending on the cooling speed. Thin sections were cut from the centre of the injected moulded bars through microtoming for MWCNT loadings of 0 and 1 wt%. The sections were placed between two glass slides and kept in an oven at 175 °C for 20 min to obtain a thin layer of material. To assess the effect of cooling speed on the crystallization process of PLA, the melted samples ~~have been~~[were](#) cooled down at two different cooling speeds. A first set of ~~six~~[six](#) sections was taken out from the oven and stored

1  
2  
3  
4  
5  
6  
7 in a cooled room at 15°C for 2h. The second set of samples was kept in the oven when  
8  
9 cooling the oven temperature down to ambient temperature at a slow cooling rate of  
10  
11 190 around 1°C/min. ~~Images of Pictures from~~ the films were obtained with a Axio Scope A1  
12  
13 (Zeiss), equipped with polarized light module.

14  
15 **Electrical conductivity measurements**  
16

17 The specific electrical conductivity was determined by four-point method following  
18  
19 European standard EN ISO 3915 (Figure 1), performed on rectangular samples sized 70x10x4  
20  
21 mm<sup>3</sup>. In the four-point measurement configuration the electrodes are fixed on the cut  
22 195  
23 surfaces and the sensor electrodes measuring the actual electric ~~tension-voltage~~ are  
24  
25 positioned on an unmodified surface. The advantage of this configuration is that the contact  
26  
27 quality between the shell-electrodes and the sample does not influence the electric tension  
28  
29 measured between the sensor electrodes. The four electrodes are positioned in a row  
30  
31 parallel to injection direction. The required voltage of up to 60 V was generated by the  
32 200  
33 digital DC power supply D3022 (CYE) applied by clamped shell-electrodes. Two sensor  
34  
35 electrodes were fixed at a constant distance (d) of 10 mm. ~~The ISO standard specified that~~  
36  
37 ~~sensor electrodes should be placed onto the wider side of the sample. In our case these~~  
38  
39 ~~sample surfaces were not flat enough for continuous contact of the electrodes. Therefore,~~  
40  
41 ~~the sensor electrodes were positioned on the narrower lateral side, which were sufficiently~~  
42 205  
43 ~~flat. In this configuration the maximal contact area was smaller than described in the~~  
44  
45 ~~standard. This should result in slightly lower conductivities compared to the configuration~~  
46  
47 ~~described in the standard. To limit the effect of contact variability between the sensor~~  
48  
49 ~~electrodes and the sample, four measurements were performed at different positions on the~~  
50  
51 ~~sample.~~ Three samples were measured for each MWCNT loading. The mean value of the  
52 210  
53 conductivity for each composite was obtained by averaging ~~over all the~~ measurements.  
54  
55  
56  
57  
58  
59  
60

The specific electrical conductivity  $\sigma$  was calculated using equation (2).

$$\sigma = \frac{d}{\Delta U/I \times A} \quad (2)$$

In equation (2)  $d$  is the distance between the sensor electrodes in m and  $A$  is the cross section surface of the sample in  $m^2$ . The voltage  $\Delta U$  was measured between the two sensor electrodes of a Solartron Schlumberger 7150 Digital multimeter. The current value  $I$  provided by the power supply on the circuit, was measured by an Amprobe® multimeter. This configuration measures the resistivity in the flow direction. Readings were taken after 1 min of stable current (set to values between 0.3 and 25 mA depending on sample conductivity) and stable mechanical loading on the sensor electrodes of 10 N applied by a Zwick/Roell ZmartPro. Because of the voltage source limitations it was only possible to measure specific resistivity from 1  $\Omega \cdot cm$  to 1  $k\Omega \cdot cm$ . However, this corresponded to specific conductivities between  $10^{-1}$  and  $10^2$  S/m, which includes the transition from conductive to semi conductive materials. The percolation threshold, which is usually determined at much lower conductivity ranges, could therefore not be precisely determined. [insert Figure 1.]

## RESULTS AND DISCUSSION

### Filler distribution and dispersion

Fracture surfaces of the PLA composites with increasing MWCNT loadings were investigated by SEM (Figure 2). The addition of 0.5 wt% of MWCNTs (Figure 2a) did not significantly affect the appearance of the surface and the filler could not be located. However, increasing the loading to 1 wt% rendered the fracture surface flaky (Figure 2b). The surface texture became even rougher at 5 and 10 wt% (Figure 2c and d). Even though the nanotubes could not be

Formatted: Font: (Default) +Headings (Calibri)

Formatted: Font: (Default) +Headings (Calibri), 12 pt

1  
2  
3  
4  
5  
6  
7  
8  
9  
10  
11  
12  
13  
14  
15  
16  
17  
18  
19  
20  
21  
22  
23  
24  
25  
26  
27  
28  
29  
30  
31  
32  
33  
34  
35  
36  
37  
38  
39  
40  
41  
42  
43  
44  
45  
46  
47  
48  
49  
50  
51  
52  
53  
54  
55  
56  
57  
58  
59  
60

resolved by SEM, their effect on the texture of the fracture surfaces was evident. [insert Figure 2.]

To elucidate in detail how the filler was incorporated into the polymer matrix, high-resolution AFM imaging was performed in tapping mode (Figure 3). For all tested composites containing MWCNT fibrous structures with diameters of around 20 nm could be observed. Considering the measurement error due to the comparatively large tip diameter, this was within the range of the diameter measured for the raw CNT, which suggests that the fibrous structures ~~corresponded to~~ MWCNTs. The AFM images indicated that the tubes are quite evenly distributed in the polymer matrix. Thus, it appears that for all of the investigated CNT loadings the melt processing was effective in distributing the nanotubes homogeneously in the PLA matrix.

In many of the AFM images recorded on the cross-section of the composite containing 1 wt% MWCNT the tubes appeared to be aligned (Figure 3b), whereas at 5 and 10 wt% MWCNT (Figure 3c, 3d) no preferential orientation was found. The alignment ~~could can~~ be due to flow-alignment during injection moulding but as the cuts were made perpendicular to the flow direction, the nanotubes should be oriented perpendicular to the cutting direction, ~~yet this was not the case and they were not~~. A more plausible explanation is a dragging of the MWCNTs by the microtome blade during cutting, as explained in the study of Ajayan et al.<sup>39</sup>

Unexpectedly, the microtoming dragging effect on the tubes was not observed at higher nanotube loadings. The dominating features of the 5 and 10 wt% MWCNT samples were curved tubes, and tubes that protruded from the surface (Figure 3c, g). This indicates to some degree an entanglement of the MWCNT within the samples, having 5 and 10 wt%

MWCNT, which prevented pull-out and secondary alignment of mobile MWCNTs on cut surfaces, ~~that is as~~ assumed to take place with the 1 wt% ~~loadingsamples.~~

In injection moulding filler repartitioning and reorientation may occur depending on the mould geometry and filler shape. In the case of fibrous fillers, one expects the formation of two distinct regions: a skin layer and a core region.<sup>18,21-23</sup> In the skin layer, an alignment of the fillers in injection direction is expected, due to the higher shear and quick cooling in this region.<sup>18</sup> As a result, this region is highly anisotropic. It has been found that the skin layer acts as an insulating layer when measured perpendicular to the skin layer (volume conductivity), but shows higher conductivities when measuring parallel to the plane of the skin layer.<sup>21-23</sup> ~~The~~ Our AFM imaging ~~result~~ from the core region of the composites with CNT loadings of 5 wt% and higher (Figure 3 c and d) ~~They~~ indicate interconnection without flow alignment, and ~~with~~ no dragging alignment due to cutting. This suggests that tube/tube contacts and MWCNT entanglement may inhibit the ordering and alignment in the skin layer, thereby improving electron transport into the material through the skin layer.

In the AFM images presented in Figure 3, the nanotubes appear distinct from the polymer matrix. Yoon et al.<sup>32</sup> described that the boundary between the PLA-grafted MWCNT and the PLA matrix was less discernible on the scanning electron microscopy of fractured surface, compared to unmodified MWCNT. This was explained by improved wrapping of the modified MWCNT by the polymer matrix.<sup>32</sup> The clear delimitation of the MWCNT in our study is in accordance with the expected restricted interaction between the unmodified MWCNTs and the PLA matrix, which results from the difference in their surface energies. Such a structure would favour the electrical tube/tube contact and potentially increase the conductivity of the composites.



1  
2  
3  
4  
5  
6  
7  
8  
9  
10  
11  
12  
13  
14  
15  
16  
17  
18  
19  
20  
21  
22  
23  
24  
25  
26  
27  
28  
29  
30  
31  
32  
33  
34  
35  
36  
37  
38  
39  
40  
41  
42  
43  
44  
45  
46  
47  
48  
49  
50  
51  
52  
53  
54  
55  
56  
57  
58  
59  
60

In the AFM phase contrast images (Figure 3e to h) the CNTs can be clearly recognized because of their higher stiffness. It can also be seen that the stiffness of the polymer matrix increases as the proportion of filler increases. This suggests that the nanotubes might affect the mechanical properties of the matrix. [insert Figure 3.]

**Tensile strength**

To determine the effect of the interaction between the polymer and the unmodified filler the tensile strength was measured (Figure 4). As the MWCNT weight fraction increases the tensile strength decreases. At 10 wt% MWCNT loading the tensile strength was 26% lower than for neat PLA. The poor interaction between MWCNTs and PLA is a plausible explanation for the observed decrease in tensile strength. Different trends for tensile strength, for unmodified MWCNT filled thermoplastics have been reported. Novais et al.<sup>27</sup> found an increase in tensile strength of hot-pressed panels when adding 0.5 wt% of unmodified MWCNT to PLA, but a decrease in tensile strength occurred with 1 wt%, compared to the neat polymer. Andrews et al.<sup>8</sup> studied the effect of unmodified MWCNT on polystyrene films and observed a tensile strength decrease of up to 55%, when 5 vol% (approximately 7.5 wt%) of MWCNT were added. They explained the initial decrease by the poor interaction between the MWCNT and the polymer and the presence of defects in the MWCNT structure. However, between 5 to 15 vol% (7 to 22 wt%) MWCNT, the tensile strength increased until it reached the value of neat polystyrene. This was explained by a bridging effect of clustered MWCNT, which retarded the opening cracks induced by tensile stresses. Such behaviour was not observed in the present study. [insert Figure 4.]

**MWCNT nucleation effect on polymer crystallization**

DSC was used to assess the impact of unmodified MWCNT on the crystallinity of PLA in the injection-moulded parts (Figure 5). It is generally accepted that the crystallinity derived from the first heating cycle observed in DSC analysis corresponds to the thermal state obtained after injection moulding, while the second heating gives the crystallinity after a controlled cooling process.<sup>37,41</sup> As observed on Figure 5a the crystallinity measured during the first heating cycle is essentially unaffected by the MWCNT content. On the contrary, the crystallinity measured during the second heating was more than twice as high and generally increased with increasing MWCNT loading, reaching 57% crystallinity at 10 wt%. DSC curves (Figure 5b) revealed that for loadings higher than 2.5 wt% MWCNT the onset of crystallization shifted to increasingly higher temperatures. The simultaneous increase of crystallinity and temperature at the start of crystallization is typical for heterogeneous nucleation induced by a filler.<sup>31,32</sup> As this was not observed during the first heating, we conclude that any potential nucleation effect of the MWCNTs was hindered by the relatively fast cooling during injection of the melt into the moulds, which were kept at 20 °C. [insert Figure 5].

Papageorgiou et al.<sup>29</sup> ~~measured-reported~~ an increase in the crystallisation temperature but a ~~decrease in crystallinity was~~ observed a decrease in crystallinity –when adding oxidized MWCNT to PLA. They observed irregular spherulites at MWCNT surface. It is argued that the irregular spherulites have limited polymer mobility, which in turn retarded the full crystallization of the polymer matrix. Zhang et al.<sup>33</sup> compared the crystalline structures of 2 wt% MWCNT filled polypropylene (PP) and neat PP. They found that crystallinity remained between 42 and 46% when adding MWCNTs, but it is also reported that the spherulites sizes have decreased. It is concluded that MWCNT induced the formation of numerous smaller spherulites.

1  
2  
3  
4  
5  
6  
7  
8  
9  
10  
11  
12  
13  
14  
15  
16  
17  
18  
19  
20  
21  
22  
23  
24  
25  
26  
27  
28  
29  
30  
31  
32  
33  
34  
35  
36  
37  
38  
39  
40  
41  
42  
43  
44  
45  
46  
47  
48  
49  
50  
51  
52  
53  
54  
55  
56  
57  
58  
59  
60

To observe the formation of crystalline regions in the nanocomposites exposed to slow and fast cooling, polarized light microscopy was employed on films prepared from injection moulded parts. Figure 6 presents the images of cuts prepared from neat PLA, and PLA mixed with 1 wt% nanotubes. No crystallization was observed for the films when cooled quickly from 175 °C to 15°C, which is similar to the situation during injection moulding. In contrast, the slow cooling rate of 1°C/min led to a higher degree of crystallization. Comparing the slowly cooled samples containing pure PLA with those with 1 wt% of MWCNTs, it is apparent that the presence of the nanotubes ~~have~~ reduced the spherulites sizes significantly (Figures 6 a' and b'). This is consistent with the assumption that MWCNT induced heterogeneous nucleation as observed by Zhang et al.<sup>33</sup> In summary, it was observed that in the current work our samples MWCNTs can indeed nucleate PLA spherulites and induce a higher crystallinity than ~~the one that~~ reached with larger-sized spherulites in pure PLA provided ~~the~~ the cooling rate is low small enough. [insert Figure 6.]

**Crystallinity and impact strength**

In addition to the determination of crystallinity, we performed unnotched Charpy impact strength measurements (Figure 7). At loadings of 1 wt% and above the impact strength seemed to be about 10.% higher compared to lower loadings and pure PLA. However, due to the relatively large standard deviation values no unambiguous trend could be identified. MWCNT may affect the impact strength of composites in various ways, as reported in the literature. Prashanta et al.<sup>40</sup> observed a decrease of unnotched Charpy impact strength and a slight increase of the notched Charpy impact strength measurement when adding MWCNT. They concluded that MWCNTs in polypropylene limit crack propagation, while their aggregates support crack initiation. Contrarily, Mack et al.<sup>22</sup> measured a decrease in ~~of~~

notched impact strength when the loading of unmodified MWCNT added to polycarbonate was increased.<sup>22</sup>

In line with these studies and based on the resistance to tube pull-out, observed by AFM, it seems likely that the slightly increased impact strength at higher MWCNT loadings ~~may~~ results from the bridging effect and the resulting hindrance of crack propagation. The fact that no decrease ~~of~~ in the impact strength was observed is consistent with our earlier observation of good dispersion and a low degree of aggregated MWCNT in the matrix.

[insert Figure 7.]

### Electrical properties

The electrical conductivities of the composites were measured using a four-point bulk conductivity measuring technique (see Figure 1). The specific electrical conductivities calculated from the resistivity measurement are plotted in the Figure 8. The system used for this study was capable of measuring specific conductivities between  $10^{-1}$  and  $10^3$  S/m. An arbitrary value of 0 S/m was assigned to the composites of 2.5 wt% MWCNT loading and lower as no conductivity was registered with the available equipment. Starting at 5 wt% loading MWCNT reinforced PLA was found to be electrically conductive ( $\sigma > 10^{-3}$  S/m). This indicates that the percolation threshold is located at a loading of less than 5 wt%. The conductivity increased with no levelling off to 51.7 S/m at 10 wt% MWCNT loading which was the highest loading measured. These results are consistent with the existence of interconnected MWCNT networks observed by AFM imaging at 5 and 10 wt% MWCNTs (see Figure 3) and the increase of the density of these networks with the increasing MWCNT loading.

1  
2  
3  
4  
5  
6  
7 The achieved conductivities in the present study are comparable with the highest  
8  
9 370 conductivities measured for the composites produced with entangled MWCNT and with the  
10  
11 ones reported in Bauhofer and Kovacs.<sup>42</sup> Based on a comparison of 150 different types of  
12  
13 polymer-CNT composites, these authors suggested that the electrical percolation and the  
14  
15 maximum conductivities are more influenced by the polymer type and the dispersion  
16  
17 method than by the CNT type and the production method.<sup>42</sup> Table 1 lists data from studies  
18  
19 375 dealing with unmodified and probably entangled MWCNT in thermoplastics and dispersed  
20  
21 by extrusion as well as studies on copper particles or carbon black filled thermoplastics. The  
22  
23 ~~achieved conductivities are comparable to those measured by others for biopolymer~~  
24  
25 ~~thermoplastics with similar electrical conductivities (Table 1 and Figure 9). Our results were~~  
26  
27 ~~within the ranges of other unmodified MWCNT filled thermoplastic polymers, all presenting~~  
28  
29 380 ~~relatively high conductivities when compared to MWCNT filled nanocomposites obtained~~  
30  
31 ~~after melt mixing (Figure 9).~~<sup>22,27;44-46;49-50</sup> The conductivity of ~~the composites in this work~~  
32  
33 ~~samples~~ was found to be 30% higher than the conductivity measured by Moon et al.<sup>26</sup> for  
34  
35 thin composite films containing 10 wt% MWCNT in PLA. To disperse the nanotubes within  
36  
37 the polymer matrix they used ultrasonication, which is usually described as a very good  
38  
39 385 method to disperse MWCNTs, and obtain random orientation of the filler after solvent  
40  
41 evaporation.<sup>17</sup> However, this method is more laborious and of lesser industrial relevance  
42  
43 than the melt processing that was applied here. Another difference between the  
44  
45 measurements by Moon et al.<sup>26</sup> and the current approach is that they measured surface  
46  
47 conductivity but expressed their results in S/m, which indicates volume conductivity, thus  
48  
49 390 leaving some uncertainty.

51  
52 Another study on PLA filled with unmodified MWCNTs by Novais et al.<sup>27</sup> presents  
53  
54 conductivities significantly lower than ~~our own the~~ data reported here (Figure 9). However,  
55  
56  
57  
58  
59  
60

Formatted: Superscript

Formatted: Superscript

these lower ~~values~~ ~~results~~ might at least partly be due to the two-point method used by these authors. Indeed, if the contact between the electrodes and the surface of the composites in the two-point method is not ~~optimal~~ ~~perfect~~, the resulting contact resistance is added to the composite resistance.<sup>24</sup> Interestingly, they observed ~~similar~~ ~~percolation threshold but~~ much lower conductivities for PLA-grafted MWCNTs compared to unmodified MWCNTs. This is in agreement with the hypothesis that a layer of grafted molecules can reduce the quality of the tube/tube contacts and therefore the conductivity of the network.

Some studies involving other biopolymers are listed in Table 1.<sup>22,26,27 42-4452</sup> For example, Hornbostel et al.<sup>423</sup> reported that single-wall carbon nanotube (SWCNT) filled polycarbonate (PC) films reached the percolation threshold at concentrations between 0.5 and 2 wt%, which is comparable to what we expect for our materials. However, the obtained conductivities were generally lower. This may be due to the notorious difficulty of dispersing SWCNTs and a higher degree of entanglement as compared to MWCNTs. Also, in general, the conductivity of ~~their injection moulded~~ MWCNT filled polycarbonate was lower than that of MWCNT filled PLA. This could be caused by the higher affinity and thereby more efficient embedment of MWCNTs in polycarbonate or may be due to the lower electrical conductivity of pure polycarbonate. Both effects would increase the tube/tube contact resistance.

In the study of Mack et al.<sup>22</sup> the conductivity of injection moulded MWCNT-PC parts was compared to that of extruded strands. The authors explain the much higher conductivities of the strands by a flow alignment of the filler and the absence of a skin layer at the contact between the electrodes and the extruded samples. In the present study, the conductivity was measured in the direction parallel to the flow during injection. Thus, ~~flow alignment~~ may have contributed to the higher conductivity observed ~~in our samples~~ ~~comparisone~~ to

1  
2  
3  
4  
5  
6  
7 other studies where the CNT are differently oriented as in films, for example.<sup>26</sup> [Insert  
8  
9 ~~f~~Figure 8, Table 1 and [Figure 9](#).]

11 **CONCLUSIONS**

12  
13  
14 This study demonstrates that competitive eco-friendly and electrically conductive plastics  
15  
16 can be produced by melt mixing of unmodified MWCNTs with PLA followed by injection  
17 420 moulding. At 10 wt% MWCNT a conductivity of 51 S/m was achieved, which  
18  
19 ~~correlates~~[compares](#) well with the results of other studies at laboratory scale. SEM and AFM  
20  
21 observations demonstrated that this processing methodology distributes and disperses the  
22  
23 MWCNT very well in the PLA matrix leading to percolation of a conductive network at  
24  
25 loadings below 5 wt%. However, the decrease ~~in~~[of](#) the composite tensile strength with the  
26  
27 425 addition of MWCNT showed that the unmodified MWCNT did not strongly interact with the  
28  
29 PLA and no nucleation effect of the MWCNT on the PLA crystallization was detected after  
30  
31 injection moulding. Crystallinity was only between 10 and 20 %. This was attributed to the  
32  
33 fast cooling after injection moulding ~~whereas~~[at](#) lower cooling rates unmodified MWCNT  
34  
35 were found to nucleate PLA crystallization and reached ~~ed~~ much higher crystallinities, e.g. 57 %  
36  
37 430 at 10 wt% MWCNTs.  
38  
39  
40  
41

42 **ACKNOWLEDGEMENTS**

43  
44  
45 We gratefully acknowledge the assistance of the Institute of Wood Technology and  
46  
47 Renewable Materials, and the Institute of Natural Materials Technologies of the BOKU-  
48  
49 435 University of Natural Resources and Life Sciences of Vienna. We also thank Ines Fritz  
50  
51 (Institute of Environmental Biotechnology), Pum Dietmar (Department of  
52  
53 Nanobiotechnology) and the Institute of Physics and Material Sciences of BOKU. We further  
54  
55  
56  
57  
58  
59  
60

thank Dr. Soledad Peresin for initiating and the Cost Action FP 1105 for providing funding for the co-operation between Dr. T. Nypelö, Dr. H. Bock and P. Rivière. The companies NatureWorks® and C-polymers are acknowledged for providing [the](#) raw materials. G. Frieling from the Technical University of Dortmund, Prof. Achim Walter Hassel from the Johannes Kepler University Linz, and Dorothea Schwarz from DEKRA EXAM GmbH are acknowledged for their help with the electrical conductivity measurements.

#### Funding acknowledgments:

The presented study received substantial financial support by the Government of Lower Austria.

#### REFERENCES

1. Avella M, Buzarovska A, Errico ME, et al. Eco-Challenges of Bio-Based Polymer Composites. *Materials* 2009; 2: 911-925.
2. Lagaron JM and Lopez-Rubio A. Nanotechnology for bioplastics: opportunities, challenges and strategies. *Trends in Food Science & Technology*. 2011; 22: 611-617.
3. European Bioplastics and Institute for Bioplastics and Biocomposites. Bioplastics market grows above average between 2012 and 2017. [www.en.european-bioplastics.org/wp-content/uploads/2013/12/EuBP\\_market\\_data\\_2012.pdf](http://www.en.european-bioplastics.org/wp-content/uploads/2013/12/EuBP_market_data_2012.pdf) (2013, accessed 24 June 2014).
4. Leute U. *Kunststoffe und EMV Elektromagnetische Verträglichkeit mit leitfähigen Kunststoffen*. Kontakt and Studium Band 678 expertverlag, Renningen, Germany, 2014; vol.3: p.61, 69-78, 103, 115.



5. Ramuz MP, Vosgueritchian M, Wei P, et al. Evaluation of solution processable carbon-based electrodes for all-carbon solar cells. *ACS\_NANO* 2012; ~~vol.6~~ (11); ~~no.11~~: 10384-10395.

6. Shih YF, Wang YP and Hsieh CF. Preparation and properties of PLA/long alkyl chain modified multi-walled carbon nanotubes nanocomposites. *Journal of P. Polym. Eng.ineering* 2011; ~~vol.31~~ (~~no.1~~): 13-19.

7. Paradise M and Goswami T. Carbon nanotubes - Production and industrial applications. *Mater.ials & Des.ign* 2007; 28: 1477-1489.

8. Andrews R, Jacques D, Qian D, et al. Multiwall Carbon Nanotubes: Synthesis and Application. *Acc. Chem. Res.* 2002; 35: 1008-1017.

9. Kuilla T, Bhadra S, Yao D, et al. Recent advances in graphene based polymer composites. *Progress. in Polym.er Sci.ence* 2010; 35: 1350-1375.

10. Al-Saleh MH and Sundararaj U. A review of vapor grown carbon nanofiber/polymer conductive composites. *Carbon* 2009; 47: 2-22.

11. Roy N, Sengupta R and Bhowmick AK. Modifications of carbon for polymer composites. *Prog.ress in Polym.er Sci.ence* 2012; 37: 781-819.

12. Iijima S. Helical microtubules of graphitic carbón. *Nature* 1991; 354: 56-58

13. Velasco- Santos C, Martinez-Hernandez AL and Castano VM. Carbon nanotube-polymer nanocomposites: The role of interfaces. *Compos.ite Interfaces* 2005; ~~vol.11~~; ~~no. (8-9)~~: 567-586.

14. Costa P, Silva J, Ansón-Casaos A, et al. Effect of carbón nanotube type and functionalization on the electrical, thermal, mechanical and electromechanical properties of carbon nanotube/styrene-butadiene-styrene composites for large strain sensor applications. *Composites: Part B* 2014; 61: 136-146.

- 1  
2  
3  
4  
5  
6  
7 15. Villmow T, Pötschke P, Pegel S, et al. Influence of twin-screw extrusion conditions on  
8 the dispersion of multi-walled carbon nanotubes in a poly(lactic acid) matrix. *Polymer*  
9 2008; 49: 3500-3509.  
10 485  
11  
12  
13 16. Pegel S, Pötschke P, Petzold G, et al. Dispersion, agglomeration, and network  
14 formation of multiwalled carbon nanotubes in polycarbonate melts. *Polymer* 2008;  
15 49: 974-984.  
16  
17  
18  
19 17. Byrne MT and Gun'ko YK. Recent Advances in research on Carbon Nanotube-Polymer  
20 Composites. *Adv. Mater.* 2010; 22: 1675-1688.  
21 490  
22  
23 18. Villmow T, Pegel S, Pötschke P, et al. Influence of injection moulding parameters on  
24 the electrical resistivity of polycarbonate filled with multi-walled carbon nanotubes.  
25  
26  
27 *Composites Science and Technology* 2008; 68: 777-789.  
28  
29  
30 19. Aguilar JO, Bautista-Quijano JR and Avilés F. influence of carbon nanotube clustering  
31 on the electrical conductivity of polymer composite films. *EXPRESS Polym. Letters*  
32 495  
33 2010; Vol. 4, No. (5): 292-299.  
34  
35  
36 20. Valentino O, Sarno M, Rainone NG, et al. Influence of the polymer structure and  
37 nanotube concentration on the conductivity and rheological properties of  
38 polyethylene/CNT composites. *Physica E* 2008; 40: 2440-2445.  
39  
40  
41 500 21. Nobile MR, Simon GP, Valentino O, et al. Rheological and Structure Investigation of  
42 Melt Mixed Multi-Walled Carbon nanotube/PE Composites. *Macromol. Symp.* 2007;  
43 247: 78-87  
44  
45  
46  
47 22. Mack C, Sathyanarayana S, Weiss P, et al. Twin-screw extrusion of multi walled  
48 carbon nanotubes reinforced polycarbonate composites: Investigation of electrical  
49 and mechanical properties. In: International Conference on Structural Nano  
50  
51  
52 505  
53  
54  
55  
56  
57  
58  
59  
60

Composites (ed. Materials Science and Engineering), Bedford, United Kingdom, 2012, vol. 40.

23. Thomas S, Joseph K, Malhotra SK, et al. *Polymer Composites, Macro- and Microcomposites*. 1th ed. Weinheim Germany: Wiley-VCH Verlag&Co. KGaA, 2012, vol.1, p.113.

24. Guoquan W. Electrical Resistance Measurement of Conductive Network in Short Carbon Fibre-Polymer Composites. *Polym. Test.* 1997; 16: 277-286.

25. Kuan CF, Kuan HC, Ma CCM, et al. Mechanical and electrical properties of multi-wall carbón nanotube/poly(lactic acid) composites. *J. Journal of Phys.ics and Chem.istry of Solids* 2008; 69: 1395-1398.

26. Moon SI, Jin F, Lee CJ, et al. Novel Carbon Nanotube/Poly(L-lactic acid) nanocomposites; Their Modulus, Thermal Stability, and Electrical Conductivity. *Macromol. Symp.* 2005; 224: 287-295.

27. Novais RM, Simon F, Pötschke P, et al. Poly(lactic acid) composites with poly(lactic acid modified carbon nanotubes. *J. Journal of Polym. Science Part A: Polymer Chemistry* 2013; 51: 3740-3750.

28. Li H and Huneault MA. Effect of nucleation and plasticization on the crystallization of poly(lactic acid). *Polymer* 2007; 48: 6855-6866.

29. Papageorgiou GZ, Achilias DS, Nanaki S, et al. PLA nanocomposites: Effect of filler type on non-isothermal crystallization. *Thermochim. Acta* 2010; 511: 129-139.

30. Spitalsky Z, Tasis D, Papagelis K, et al. Carbon nanotube-polymer composites: Chemistry, processing mechanical and electrical properties. *Prog.ress in Polym. Science* 2010; 35: 357-401.

31. Tsuji H, Kawashima Y, Takikawa H, et al. Poly(L-lactide)/nano-structured carbon  
composites: Conductivity, thermal properties, crystallization, and biodegradation.  
*Polymer* 2007; 48: 4213-4225.
32. Yoon JT, Jeong YG, Lee SC, et al. Influences of poly (lactic acid)-grafted carbon  
nanotube on thermal, mechanical, and electrical properties of poly(lactic acid).  
*Polym.ers Adv.anced Technol.egies* 2009; 20: 631-638.
33. Zhang H and Zhang Z. Impact behaviour of polypropylene filled with multi-walled  
carbon nanotubes. *Eur.opean Polym.er Journa.l* 2007; 43: 3197-3207.
34. Cadek M, Coleman JN, Ryan KP, et al. Reinforcement of Polymers with Carbon  
Nanotubes: The Role of Nanotube Surface Area. *Nano.lett.ers* 2004; ~~vol.4, No. (2):~~  
353-356.
35. Alig I, Lellinger D, Dudkin SM, et al. Conductivity spectroscopy on melt processed  
polypropylene-multiwalled carbon nanotube composites: recovery after shear and  
crystallization. *Polymer* 2007; 48: 1020-1029.
36. Magonov SN, Elings V and Whangbo MH. Phase imaging and stiffness in tapping  
mode atomic force microscopy. *Surf.ace Sci.ence* 1997; ~~vol.375-(2-3):~~ 385-391.
37. Sichina WJ. DSC as Problem Solving Too: Measurement of Percent Crystallinity of  
Thermoplastics. Perkin Elmer<sup>TM</sup> Instruments, Thermal analyses Application note,  
[http://www.perkinelmer.com/Content/applicationnotes/app\\_thermalcrystallinitythe](http://www.perkinelmer.com/Content/applicationnotes/app_thermalcrystallinitythermoplastics.pdf)  
[rmoplastics.pdf](http://www.perkinelmer.com/Content/applicationnotes/app_thermalcrystallinitythermoplastics.pdf) (accessed July, 10. 2014)
38. Gregorova A, Hrabalova M, Wimmer R, et al. Poly(lactide acid) Composites  
Reinforced with Fibers Obtained from different Tissues Types of *Picea sitchensis*  
*J.ournal of Applied. Polym.er Sci.ence* 2009; 114: 2616-2623.

39. Ajayan PM, Stephan O, Colliex C, et al. Aligned Carbon Nanotube Arrays Formed by Cutting a Polymer Resin—Nanotube Composite. *Science* 1994, 5176: 1212-1214.  
<http://www.sciencepubs.org/content/265/5176/1212-abstract>

40. Prashantha K, Soulestin J, Lacrampe MF, et al. Masterbatch-based multi-walled carbon nanotube filled polypropylene nanocomposites: Assessment of rheological and mechanical properties. *Compos. Sci. Technol.* 2009; 69: 1756-1763.

41. Gregorova A. Application of Differential Scanning Calorimetry to the Characterization of Biopolymers, In: Dr. Amal Ali Elkordy (Ed.) *Applications of Calorimetry in a Wide Context - Differential Scanning Calorimetry, Isothermal Titration Calorimetry and Microcalorimetry*. 2013, pp. 3-20.

42-43. Bauhofer W, Kovacs J S. A review and analysis of electrical percolation in carbon nanotube polymer composites. *Compos. Sci. Technol.* 2009; 69 (10): 1486-1498.

42-43. Hornbostel B, Pötschke P, Kotz J, et al. Single-walled carbon nanotubes/polycarbonate composites: basic electrical and mechanical properties. *Phys. Rev. B* 2006; vol. 243, No. (13): 3445-3451.

44. Pötschke P, Abdel-Goad M, Alig I, Dudkin S, Lellinger D. Rheological and dielectrical characterization of melt mixed polycarbonate-multiwalled carbon nanotube composites. *Polymer* 2004; 45 (26): 8863-8870.

45. Pötschke P, Dudkin SM, Alig I. Dielectric spectroscopy on melt processed polycarbonate-multiwalled carbon nanotube composites. *Polymer* 2003; 44 (17): 5023-5030.

Formatted: Font: Italic

Formatted: Font: Italic

Formatted: Font: Italic

Formatted: Font: Italic

Formatted: German (Austria)

Formatted: Font: Italic

46. Pötschke P, Fornes TD, Paul DR. Rheological behavior of multiwalled carbon nanotube/polycarbonate composites. *Polymer* 2002; 43 (11): 3247-3255.
- 43-47. Merzouki A and Haddaoui N. Electrical Conductivity Modeling of Polypropylene Composites Filled with Carbon Black and Acetylene Black. *International Scholarly Research Notices* ~~NR~~ *Polymer Science* 2012; ~~7~~.
48. Kharchenko SB, Douglas JF, Obrzut J, et al. Flow-induced properties of nanotube-filled polymer materials. *Nat. Mater.* 2004; 3 (8): 564-568.
49. Tjong SC, Liang GD and Bao SP. Electrical behaviour of polypropylene/multiwalled carbon nanotube nanocomposites with low percolation threshold. *Scr. Mater.* 2007; 57 (6): 461-464.
50. Meincke O, Kaempfer D, Weickmann H, et al. Mechanical properties and electrical conductivity of carbon-nanotube filled polyamide-6 and its blends with acrylonitrile/butadiene/styrene. *Polymer* 2004; 45 (3): 739-748.
51. Kodgire PV, Bhattacharyya AR, Bose S, Gupta N, Kulkarni AR, Misra A. Control of multiwall carbon nanotubes dispersion in polyamide6 matrix: an assessment through electrical conductivity. *Chem. Phys. Lett.* 2006; vol. 432, 4-6: 480-485.
52. Markov AV, Bock HJ, Mauser A et al. Injection moulded copper filled thermoplastics for the product development. *Material-Wwiss. u. Werkstofftech.* 2007; vol. 38, No. (10): 836-841.
- 44.

Formatted: Font: Italic

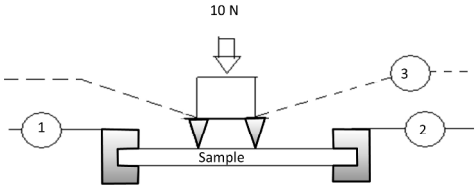
Formatted: Font: Italic

Formatted: German (Austria)

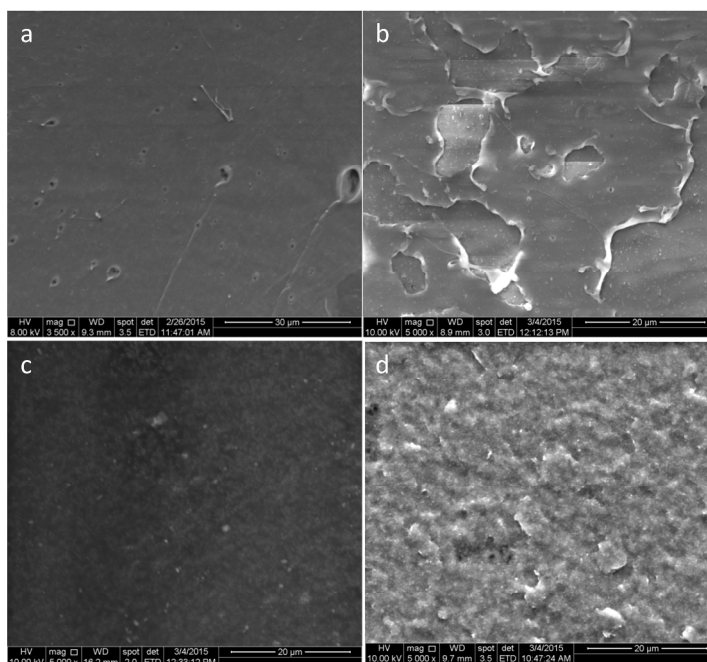
Formatted: Font: Italic

Formatted: English (U.K.)

Formatted: Left, Indent: Left: 0.5", Space After: 10 pt, Line spacing: single, No bullets or numbering



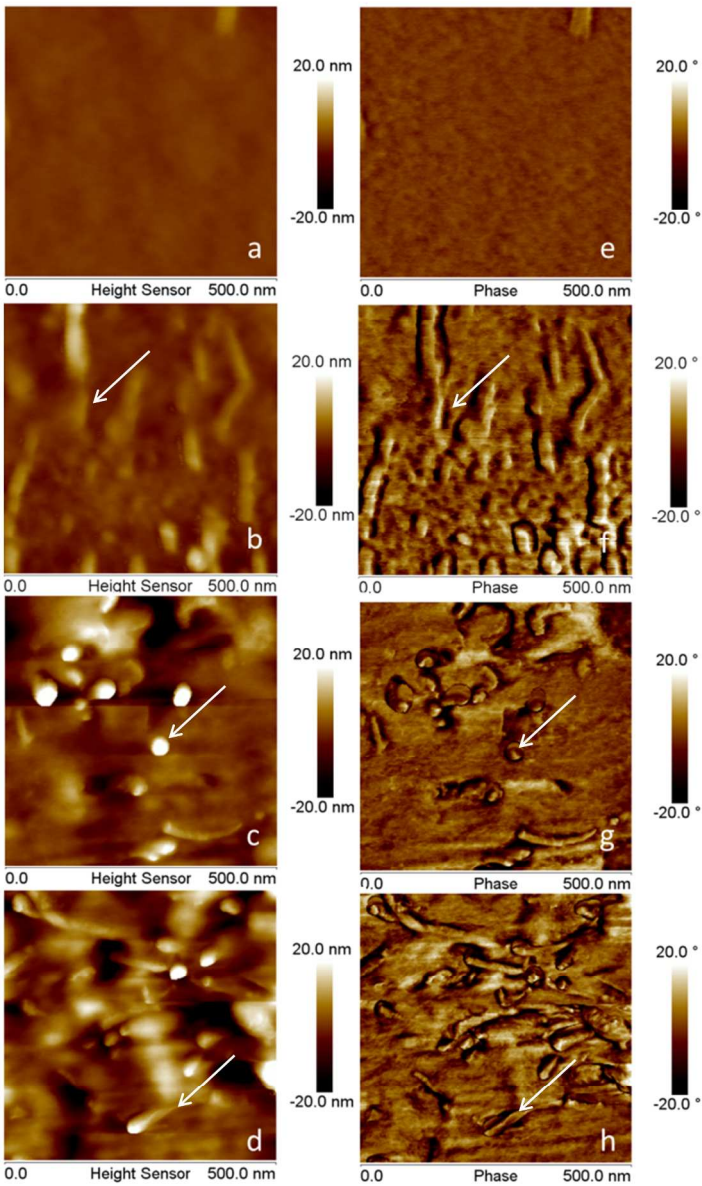
Installation of electrical conductivity determination, 1 is the voltage source, 2 the ammeter and 3 corresponds to the multimeter in the voltmeter mode. The electrodes are represented in grey colour.  
254x190mm (300 x 300 DPI)



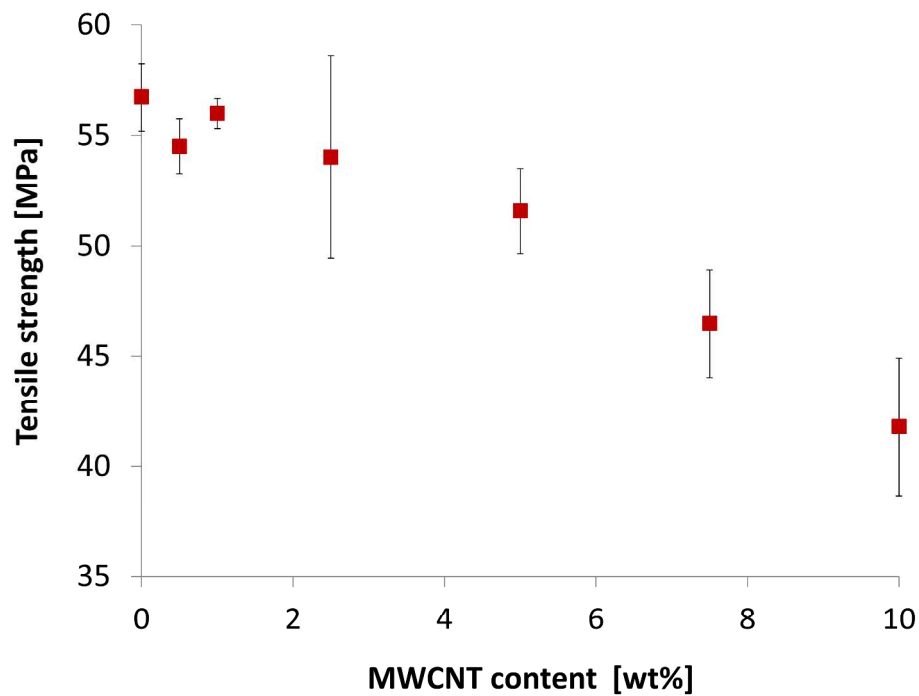
Scanning electron microscopy images of the fracture surface of PLA with a) 0.5, b) 1, c) 5 and d) 10 wt% MWCNT loading. The image (a) was recorded after applying a gold coating on the surface; the others images were recorded without gold coating. The scale bar in each image corresponds to 20 µm.

254x190mm (300 x 300 DPI)

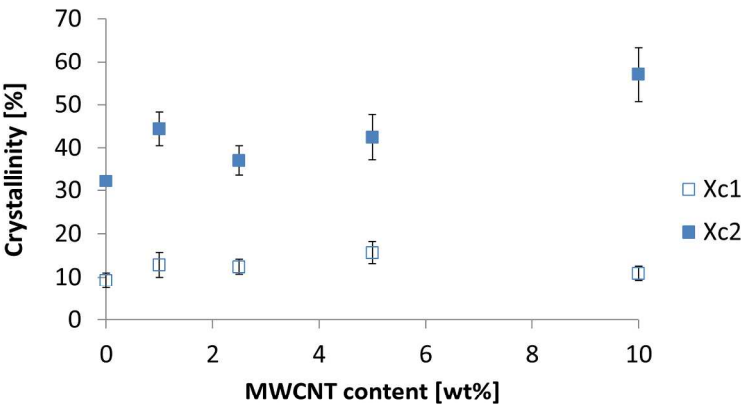




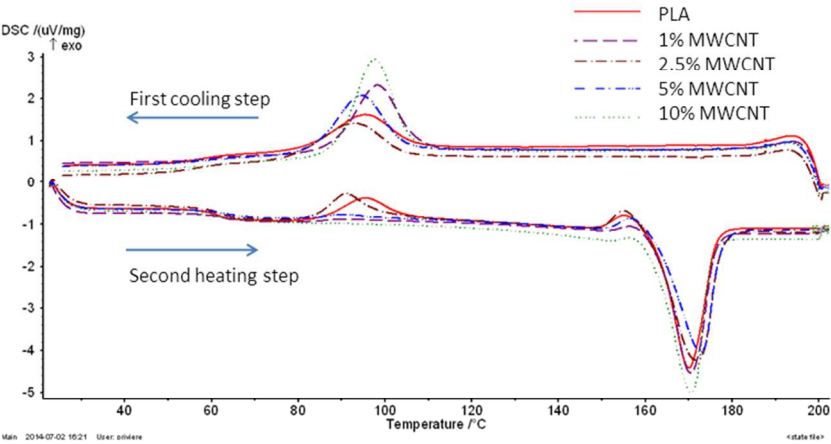
AFM topography (a-d) and corresponding phase images (e-h) recorded in tapping mode showing a section of 0.25  $\mu\text{m}^2$  of the PLA composite with 0 (a, e), 1 (b, f), 5 (c, g) and 10 (d, h) wt% MWCNT. The arrows indicate MWCNT location. The cutting direction of the microtome is for every picture from the right to the left.  
190x254mm (300 x 300 DPI)



Mean tensile strength of 10 samples with corresponding standard deviation for each composite based on PLA at different MWCNT loadings.  
254x190mm (300 x 300 DPI)



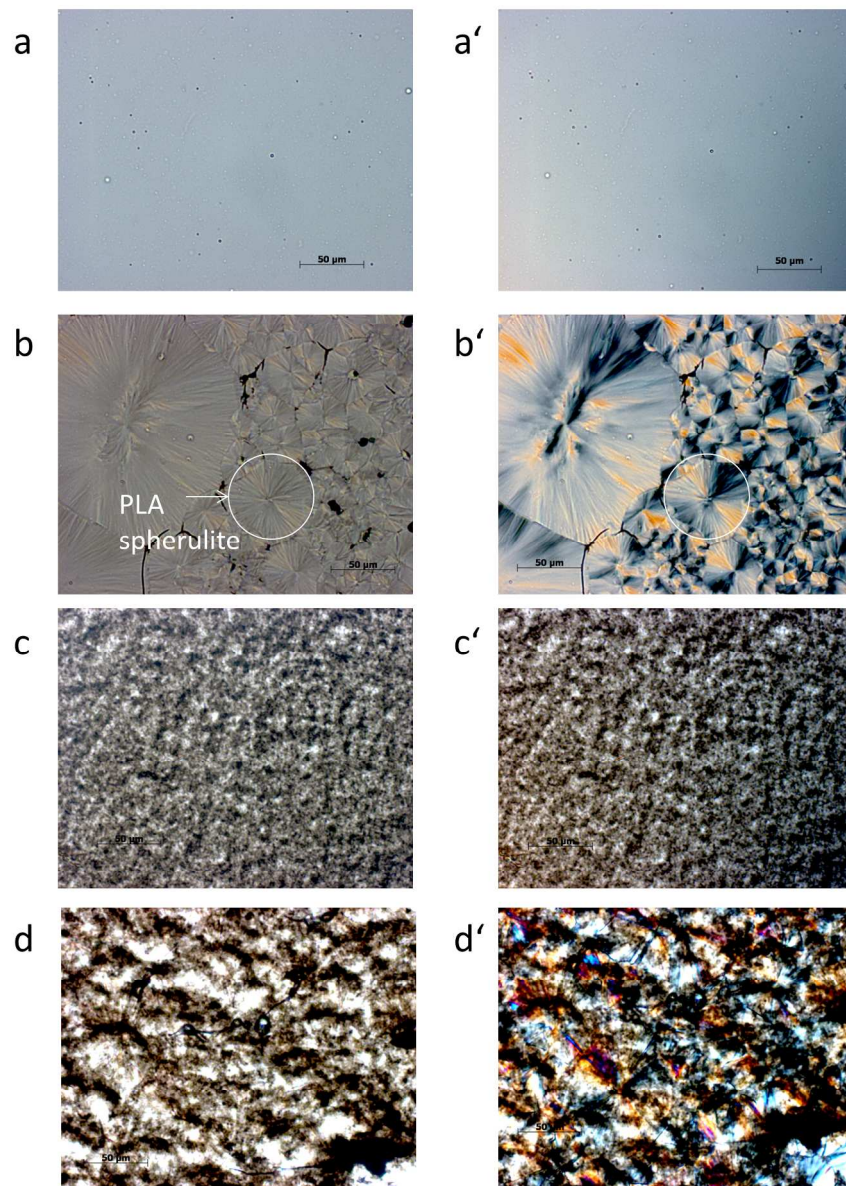
5. a



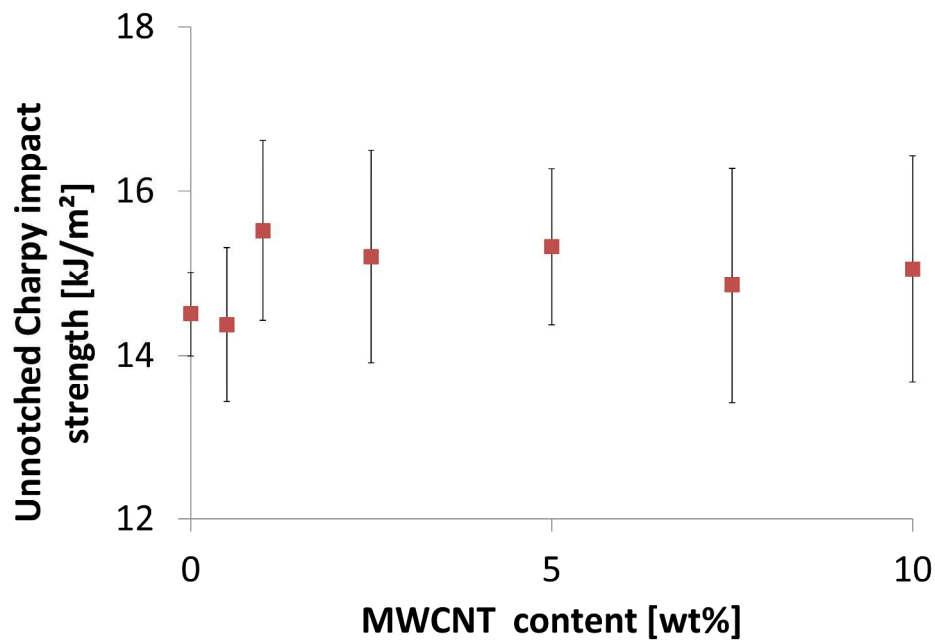
5. b

Crystallinity of injection moulded PLA samples with 0-10 wt% MWCNT loading (a) calculated from DSC thermograms of first (Xc1) and second (Xc2) heating steps. The values are an average of three samples for each composite. The DSC thermograms on (b) show the first cooling step and the second heating step reflecting the nucleation effect of MWCNT on PLA obtained at low cooling rate.

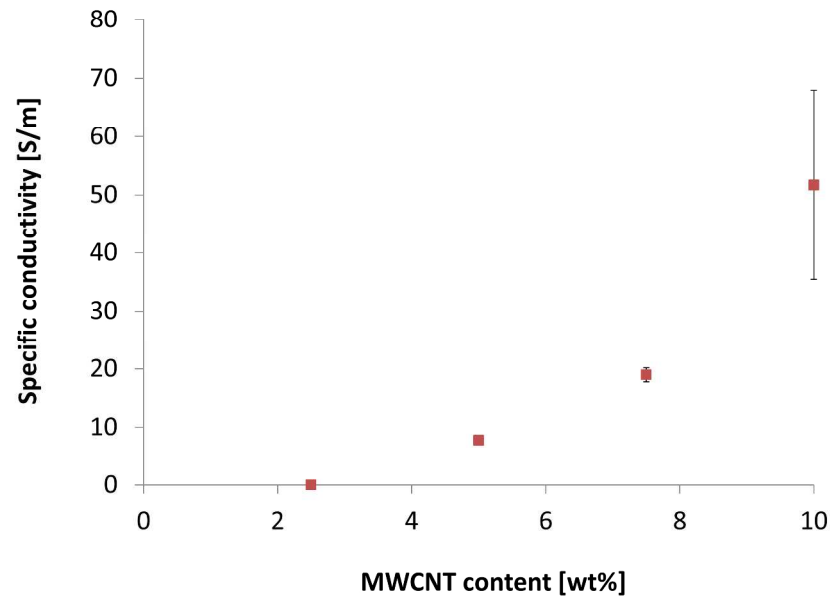
190x254mm (300 x 300 DPI)



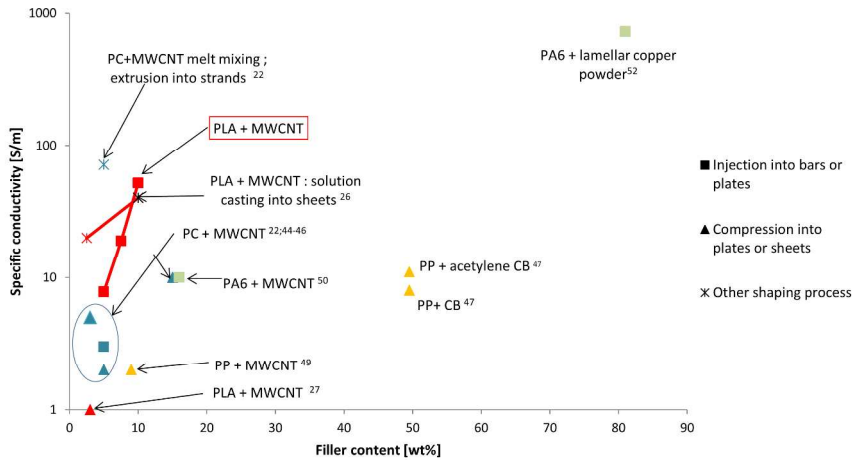
Microscopic analysis of crystalline structure of pure PLA films (a, a' and b, b') and PLA films with 1 wt% MWCNT (c, c' and d, d'), exposed directly from 175 °C to 15 °C (a, a' and c, c') and under cooling rate lower than 1 °C/min, (b, b' and d, d'). The image pairs correspond to observation under non-polarized light (x) and under polarized light (x'). One PLA spherulite was circled in white on b and b' pictures. All pictures are taken at the same magnification with the scale bar as shown in (a) corresponding to 50 μm.  
190x254mm (300 x 300 DPI)



Charpy unnotched impact strength of the PLA composite with 0-10 wt% MWCNT loadings. The mean and standard deviation values are from 10 samples for each MWCNT loading.  
254x190mm (300 x 300 DPI)



Specific volume conductivity of MWCNT loaded PLA composites from four measurements on three samples for each composite.  
254x190mm (300 x 300 DPI)



Comparison of the electrical performance of the composites produced in this study (boxed) with previously published works (See list of references for the cited publications in Table 1). The legend indicates the moulding process used after melt mixing (compression or injection moulding). If a different process was used it is described in the data label.

254x190mm (300 x 300 DPI)



Formulation			Methods		Results			ref.
Polymer		Filler type	Production of the samples	Measurement method	Percolation threshold [wt%]	Maximal content tested [wt%]	Maximal conductivity [S/m]	
Type	Conductivity [S/m]							
PLA	10 <sup>-14</sup>	MWCNT	Bars after melt mixing and injection moulding	Four-point DIN EN ISO 3915(10N) parallel to the injection flow	<5	10	51.7	current result
PLA	10 <sup>-14</sup>	MWCNT	Sheets after ultrasonication in chloroforme and evaporation	Surface four-point method	0-2.5	10	40	26
PLA	10 <sup>-14</sup>	MWCNT	Plates after melt mixing and compression moulding	Volume conductivity two-point method	0.5	3	1	27
PLA	10 <sup>-14</sup>	PLA-grafted MWCNT	Plates after melt mixing and compression moulding	Volume conductivity two-point method	0.5	3	Around 0.032	27
PC	10 <sup>-17</sup>	MWCNT	Bars from melt mixing and injection moulding	n.a.	1	5	3	22
PC	10 <sup>-17</sup>	MWCNT	Strands extruded after melt mixing	n.a.	1	5	71	22
PC	~10 <sup>-16</sup>	SWCNT	Plates from melt mixing and compression moulding	DIN EN ISO 3915 perpendicular to pressing	0.5-2 (ring electrodes IEC 93:1980)	10	10 <sup>-1</sup> (to 10 if precoagulation)	43
PC	~10 <sup>-15</sup>	MWCNT	Sheets after melt mixing and compression moulding	Volumetric two-point method In the compression direction	1	12.5	5 (at 3 wt% loading)	44
PC	10 <sup>-14</sup>	MWCNT	Sheets after melt mixing and compression moulding	Volumetric two-point method In the compression direction	1.44	5	2	45
PC	10 <sup>-11</sup>	MWCNT	Bars after melt mixing and compression moulding	Volumetric two-point method Perpendicular to the compression direction	2	15	10	46
PP	10 <sup>-15</sup>	CB and acetylene CB (aCB)	Bars cut from plates after melt mixing and compression moulding	Volumetric two-point method In the compression direction	CB: 5 (2.6 vol%) aCB: 9.8 (5.3 vol%)	49.5 (30 vol%)	CB: 8 aCB: 11	47
PP	10 <sup>-9</sup>	MWCNT	Melt mixing	-	0.02 (0.01 vol%)	0.3 (0.15 vol%)	10 <sup>-1</sup>	48
PP	10 <sup>-8</sup>	MWCNT	Plates (1mm thick) from melt mixing and compression moulding	Volumetric two-point method in the compression direction	0.44 (0.22 vol%)	9 (4.5 vol%)	2	49
PA 6	~10 <sup>-13</sup>	MWCNT	Bars after melt mixing and injection moulding	Volumetric two-point method perpendicular to the injection direction	3-7	16	10	50
PA 6	~10 <sup>-12</sup>	MWCNT	Sheets after melt mixing and compression moulding	-	2.5	4	10 <sup>-1</sup>	51
PA 6	10 <sup>-14</sup>	Lamellar copper powder	Bars from plates after extrusion and injection moulding	Four-point DIN EN ISO 3915 parallel to the injection flow	77-81 (30-40 vol%)	81 (40 vol%)	730	52

PLA: polylactic acid, PC: polycarbonate, PP: polypropylene and PA6: polyamide

Comparison of electrical conductivity measurements for various composites reported in literature and in the current work. Factors differing from our measurement are bolded.

254x190mm (300 x 300 DPI)